The Astronomical Journal, 166:187 (7pp), 2023 November https://doi.org/10.3847/1538-3881/acfb01

Surrounded by Giants: Habitable Zone Stability Within the HD 141399 System

Stephen R. Kane
Department of Earth and Planetary Sciences, University of California, Riverside, CA 92521, USA; skane@ucr.edu
Received 2023 August 21; revised 2023 September 15; accepted 2023 September 17; published 2023 October 10

Abstract

The search for exoplanets has revealed a diversity of planetary system architectures, the vast majority of which diverge significantly from the template of the solar system. In particular, giant planets beyond the snow line are relatively rare, especially for low-mass stars, placing the solar system within a small category of systems with multiple giant planets at large separations. An exoplanetary system of note is that of HD 141399, consisting of a K-dwarf host star that harbors four giant planets with separations extending to ∼4.5 au. The architecture of the system creates a complex pattern of mean motion resonances and gravitationally perturbed regions that may exclude the presence of other planets, including within the habitable zone of the system. Here, we present the results of dynamical simulations that explore the interaction of the known planets of the system, their apsidal trajectories, resonance locations, and dynamical evolution. We further investigate the results of injecting Earth-mass planets and provide the regions of dynamical viability within the habitable zone where terrestrial planets may maintain long-term stability. We discuss these results in the context of the importance of giant planets for volatile delivery and planetary habitability considerations.

Unified Astronomy Thesaurus concepts: Exoplanet astronomy (486); Exoplanet dynamics (490); Exoplanet evolution (491); Exoplanet systems (484); Exoplanets (498); Orbital evolution (1178); Orbital resonances (1181); Habitable planets (695); Habitable zone (696); Astrobiology (74)

1. Introduction

The origin and evolution of planetary architectures are key areas of study within exoplanetary science. The large number of discovered planets allows a statistical analysis of these architectures and a direct comparison with the solar system (Ford 2014; Winn & Fabrycky 2015; Horner et al. 2020; Kane et al. 2021a; Mishra et al. 2023a, 2023b). In particular, we are beginning to understand the prevalence of Jupiter analogs (Wittenmyer et al. 2011, 2020; Fulton et al. 2021; Rosenthal et al. 2021), largely from the long baseline of radial velocity (RV) observations (Kane et al. 2007; Ford 2008; Wittenmyer et al. 2013). For orbits of 1–10 au, RV surveys show that giant planets are found orbiting about 6% of solar-type stars (Wittenmyer et al. 2016). Combined analysis of RV surveys, microlensing, and direct imaging surveys also shows that giant planet frequencies are likely in the 10% range for 1–100 au (Clanton & Gaudi 2016). Other combined analyses shows that the giant planet occurrence rate peaks at orbital separations of 1–3 au (Fernandes et al. 2019). Direct imaging surveys are able to probe orbits in the range 10–100 au, finding giant planets are more common around more massive host stars (Nielsen et al. 2019). The occurrence of giant planets is also correlated with other system properties, such as the metallicity of the host star (Fischer & Valenti 2005; Johnson et al. 2010; Buchhave et al. 2018) and the the presence of super-Earths (Bryan et al. 2019). However, there has been an observed dearth of Jupiter analogs around M dwarf stars (Endl et al. 2006; Pass et al. 2023), although exceptional cases have been detected (Endl et al. 2022). These insights into the occurrence of Jupiter analogs are critical for placing our solar system in a broader context of planetary architectures (Levison et al. 1998).

Planetary habitability can depend on the entire system architecture, not only in the context of volatile delivery, but also in terms of the dynamical interactions (past and present) between a planet that is a promising candidate for habitability and any other planets orbiting the same star. For example, the presence of Jupiter analogs can limit the viability of terrestrial planet occupation with the habitable zone (HZ) of the system (Kopparapu & Barnes 2010; Obertas et al. 2017; Georgakarakos et al. 2018; Hill et al. 2018; Agnew et al. 2019; Kane & Blunt 2019; Kane et al. 2020). The distribution of planetary architectures speaks to critical issues within the fields of planetary science and astrobiology, such as determining if the architecture of our solar system is typical, and the subsequent implications for volatile delivery and planetary habitability. Systems that harbor multiple giant planets are therefore of particular interest in how they may facilitate or truncate planetary habitability within the system.

Given the importance, and relative scarcity, of giant planets, a planetary system of particular interest is that of HD 141399. The host star is an early K dwarf and was found to harbor four giant planets (Vogt et al. 2014) with masses in the range ∼0.45–1.36 M_J. The planets were detected from RV observations of the host star, and so the measured planetary masses are lower limits. The system properties were further refined by Hébrard et al. (2016) and Rosenthal et al. (2021), whose increased observational baseline and improved RV precision produced a robust orbit for the outermost planet, with a period of almost 10 yr. Such a large family of giant planets is exceptionally rare, providing a useful opportunity to study the dynamics of interacting giant planets, that can often lead to scattering events and eccentric orbits (Ford & Rasio 2008; Carrera et al. 2019). The system also allows an examination of the extreme end of how giant planets and their associated orbital resonances may influence the orbital evolution of terrestrial planets.

Table 1
HD 141399 Planetary Properties

Planet	P (days)	a (au)	e	ω (°)	$M_p \sin i$ (M_J)
b	94.375	0.4176	0.053	8.0	0.452
c	201.776	0.693	0.0465	25.0	1.329
d	1074.8	2.114	0.044	297.0	1.263
e	3336	4.50	0.047	0.0	0.644

Note. Planetary properties extracted from Rosenthal et al. (2021).

In this paper, we present the results of an extensive dynamical analysis of the HD 141399 planetary system, including their orbital evolution and effect on possible terrestrial planets within the HZ. Section 2 describes the architecture and HZ of the system, as well as the locations of mean motion resonance (MMR). Section 3 presents the results of the dynamical simulations, both intrinsically for the known system architecture, and the influence of that architecture for an Earth-mass planet within the HZ. The potential further work and implications of these results for planetary habitability are discussed in Section 4, and we provide concluding remarks in Section 5.

2. System Architecture

Here we describe the HD 141399 system architecture, calculate the HZ, and provide the locations of MMR for the planets.

2.1. Orbits and Habitable Zone

The central body of the HD 141399 system consists of a K0V star (Vogt et al. 2014; Hébrard et al. 2016). We adopt the stellar mass of $M_\star = 1.091\ M_\odot$ and the planetary properties (masses and orbits) from Rosenthal et al. (2021). The masses and orbital properties of the planets are summarized in Table 1, which shows that all of the planets are more massive than Saturn and have orbits that are close to circular. Note that, since these planetary masses are derived from RV observations, these are lower limits on their true masses. Both Vogt et al. (2014) and Hébrard et al. (2016) conducted stability tests by assuming coplanarity of the orbits and decreasing the inclination of the system with respect to the plane of the sky. Their results indicate that the inclination of the system is constrained to be larger than $\sim 10^\circ$, and so the true inclination of the planetary orbits remain largely unknown.

We also calculate the HZ of the system, based upon an effective temperature of $T_{\rm eff} = 5542$ K and stellar luminosity of $L_\star = 1.637\ L_\odot$, extracted from Gaia data release 2 (Gaia Collaboration et al. 2018). The HZ may be divided into the conservative HZ (CHZ) and optimistic HZ (OHZ), the latter of which is based upon assumptions regarding the prevalence of surface liquid water for Venus and Mars (Kasting et al. 1993; Kane & Gelino 2012; Kopparapu et al. 2013, 2014; Kane et al. 2016; Hill et al. 2018, 2023). For HD 141399, the HZ regions span the ranges 1.233–2.190 au and 0.974–2.309 au for the CHZ and OHZ, respectively. The extent of the CHZ (light green) and OHZ (dark green) are shown in Figure 1, along with the orbits of the known planets. The outermost planet, planet e, lies beyond the snow line, estimated to be $\sim$3.2 au (Ida & Lin 2005; Kane 2011). Planets c and d, the most massive of the four planets, lie at either end of the HZ. In fact, the orbit of planet d is slightly eccentric such that it crosses between the outer OHZ and the outer edge of the CHZ. As such, the HZ of the system is bookended by the gravitational influence of these two giant planetary sentinels.

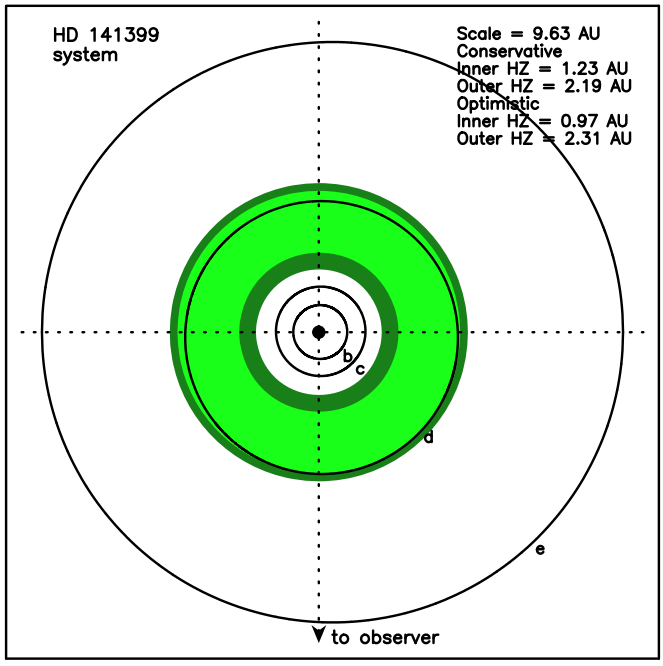

Figure 1. HZ and planetary orbits in the HD 141399 system, where the orbits are labeled by planet designation. The extent of the HZ is shown in green, where light green and dark green indicate the CHZ and OHZ, respectively. The scale of the figure is 9.63 au along each side.

2.2. Locations of Mean Motion Resonance

The periodic nature of gravitational perturbations that occur at locations of MMR result in their having special significance within complex system architectures (Petrovich et al. 2013; Hadden 2019). Such locations have been the source of numerous investigations for the solar system (Peale 1976) and exoplanetary systems (Beaugé et al. 2003; Goldreich & Schlichting 2014). MMR configurations can result from numerous formation and dynamical processes (Batygin 2015), and may even be caused by planet–planet scattering events (Raymond et al. 2008). More particularly, MMR locations can be the source of secular perturbations that may lead to dynamical instability for the associated planets (Matsumoto et al. 2012; Batygin & Morbidelli 2013).

The relative even spacing of the HD 141399 planetary orbits, combined with the high mass of the planets, produces a web of strong (low-order) MMR locations that extend out to $\sim$10 au from the host star. These MMR locations are shown in Table 2 for all four of the known planets. Of particular note are those MMR locations that align closely between different planets, such as the 1:3 MMR for planet b (0.869 au) and the 5:7 MMR for planet c (0.867 au). Also of note are the close alignments of orbital semimajor axes with MMR locations, such as the semimajor axis of planet c (0.693 au) with the 1:2 MMR for planet b (0.663 au). The MMR locations within the system will play an important role in the interpretation of the dynamical analyses for the system.

Table 2
Mean Motion Resonance Locations for the HD 141399 Planets

Planet	a (au)	3:1	5:2	7:3	2:1	3:2	7:5	5:7	2:3	1:2	3:7	2:5	1:3
b	0.4176	0.201	0.227	0.237	0.263	0.319	0.334	0.523	0.547	0.663	0.735	0.769	0.869
c	0.693	0.333	0.376	0.394	0.437	0.529	0.554	0.867	0.908	1.100	1.219	1.277	1.441
d	2.114	1.016	1.148	1.202	1.332	1.613	1.689	2.646	2.770	3.356	3.719	3.894	4.397
e	4.50	2.163	2.443	2.558	2.835	3.434	3.596	5.632	5.897	7.143	7.916	8.289	9.360

3. Dynamical Stability

Here we describe the methodology of our dynamical simulations and present the results for the known planets and an injected Earth-mass planet within the HZ.

3.1. Dynamical Simulation Methodology

The dynamical simulations conducted for our work utilized the Mercury Integrator Package (Chambers 1999), adopting the hybrid symplectic/Bulirsch-Stoer integrator with a Jacobi coordinate system, providing more accurate results for multi-planet systems (Wisdom & Holman 1991; Wisdom 2006). The time step for the integrations was set to 0.1 days to ensure adequate resolution of perturbations resulting from the inner-most planet of the system. We assumed that the orbits within the system are coplanar, and that the inclination of the orbits are such that the measured minimum planetary masses are reasonable approximations of their true masses.

The simulations were conducted in two primary configurations. First, we conducted a suite of simulations for the known planets to evaluate their long-term dynamical stability for a period of 10^8 yr. The simulations explored a range of initial orbital configurations that test semimajor axis values within the 1σ uncertainties of the values provided by Rosenthal et al. (2021). Second, we conducted an extensive suite of N-body integrations that explore the dynamical viability of an injected Earth-mass planet, similar to the methodology described by Kane (2019) and Kane et al. (2021b). Each of these integrations were run for 10^7 simulation years, significantly extending the baseline of the integrations conducted by Hébrard et al. (2016). The injected planet was placed in a circular orbit using a range of initial mean anomalies, and with semimajor axis values in the range 0.5–3.0 au, in steps of 0.005 au. This range of semimajor axes fully encompasses the HZ, described in Section 2.1. This grid of initial conditions resulted in several thousand simulations to explore orbital stability within the system HZ. The stability of the injected planet was assessed through the planet surviving the full 10^7 yr integration, where nonsurvival means that the injected planet was captured by the gravitational well of the host star or ejected from the system.

3.2. Stability of the Known Planets

Given that the system consists of four giant planets, it is important to consider angular momentum transfer that is occurring within the system, and the timescale of such interactions (Ford et al. 2001; Kane & Raymond 2014). Figure 2 shows the first 10^5 yr of a 10^8 yr simulation, indicating the nature of the gravitational perturbations within the system. The planetary orbits retain remarkable stability over the full 10^8 yr simulation, with eccentricities for all planets remaining below 0.06. The eccentricity evolution for each of the planets reveal periodic behavior over various timescales. Vogt et al. (2014) noted an angular momentum exchange between planets b and c with a period of ∼250 yr, based on a dynamical analysis of their best-fit Keplerian model at that time. To ascertain the full periodic dynamical behavior within the system, we conducted a Fourier analysis of the eccentricity evolution for each planet. We find a chain of angular momentum exchanges, starting with planets b and c whose eccentricity variations have a period of ∼327 yr. Planets c and d have eccentricity variations of ∼4070 yr, and planets d and e engage in eccentricity variations with a period of ∼25,590 yr. Some of these periodic variations may be interpreted within the context of MMR locations (Table 2) such as the near 2:1 MMR between planets b and c.

To investigate the dynamical behavior of the system further, we calculated the trajectory of the apsidal modes for four planet pairs: b–c, c–d, d–e, and c–e. Apsidal motion in the context of interacting exoplanetary systems are described by Barnes & Greenberg (2006a, 2006b), where the two basic types of apsidal behavior, libration and circulation, are separated by a boundary called a secular separatrix (Barnes & Greenberg 2006b; Kane & Raymond 2014). The apsidal trajectories for the chosen planet pairs during the initial 10^6 simulation years are represented via their polar form in Figure 3. The top-right, bottom-left, and bottom-right panels show clear indication of circulating apsidal motion for those planet pairs, since the polar trajectories consistently encompass the origin, and with no indication that they are near the separatrix transition to libration. However, the apsidal trajectories for the b–c planet pair, depicted in the top-left panel, show that they are librating, which indicates that planets b and c are indeed in or near the 2:1 MMR. Although the plots shown in Figure 3 only represent the first 10^6 yr of the full 10^8 yr simulation, we examined the evolution of both the eccentricity variations and apsidal trajectories for the remainder of the simulation data and found no significant changes in dynamical behavior.

3.3. Stability Within the Habitable Zone

Although the orbits of the four known giant planets within the HD 141399 system are exceptionally stable (see Section 3.2), they may severely limit the possibility of stable terrestrial planet orbits within the HZ. As described in Section 3.1, we tested such scenarios via a suite of planet injection simulations for an Earth-mass planet in the semimajor axis range 0.5–3.0 au. The percentage survival rates at each initial injected location are represented in the top panel of Figure 4. The extent of the HZ is depicted using the same color scheme as for Figure 1, where light green and dark green indicate the CHZ and OHZ, respectively.

As noted in Section 2.1, planets c and d are the most massive of the four known giant planets, each having masses ∼30% larger than Jupiter, and lie at either side of the HZ. As such, the gravitational influence of these planets impose significant constraints on the possible location of an injected Earth-mass planet on either side of their orbits, indicated by vertical dashed

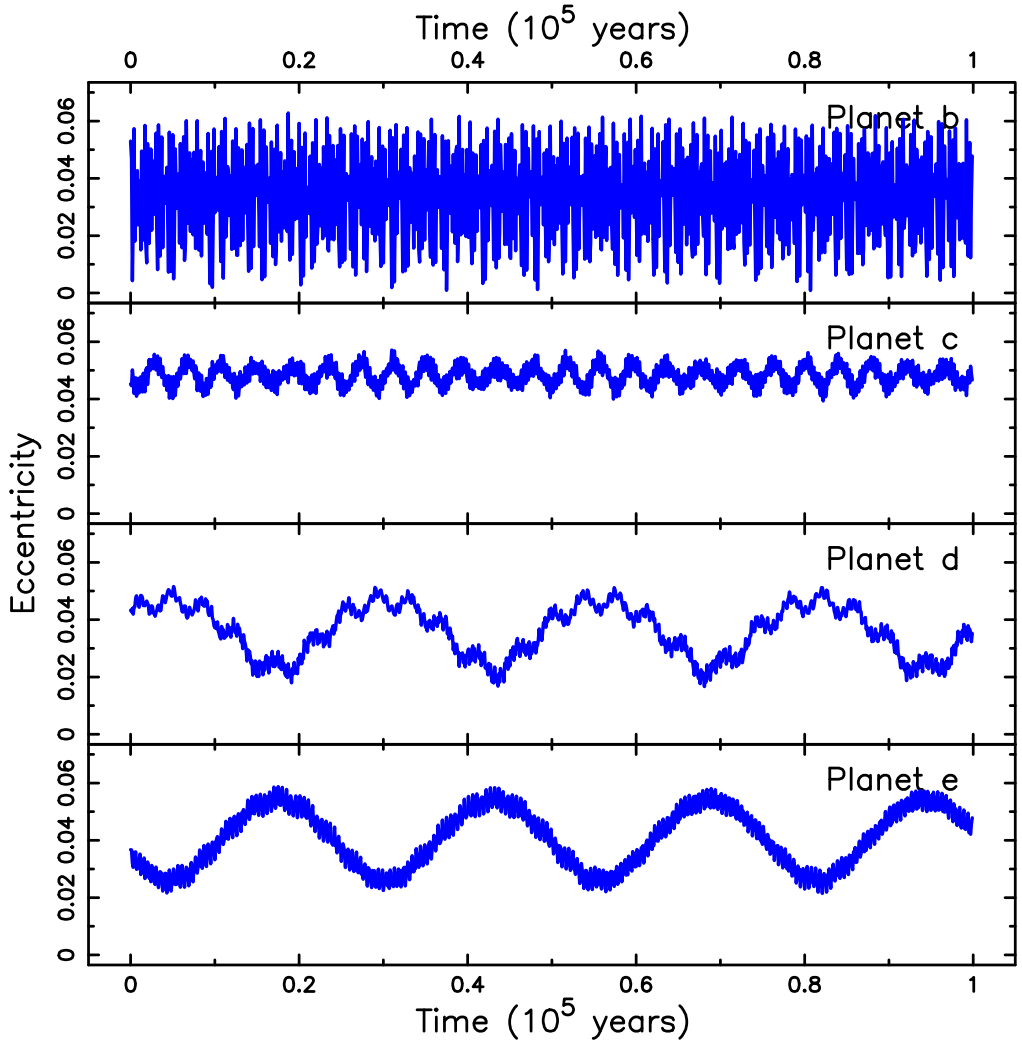

Figure 2. Eccentricity evolution for the four known planets of the HD 141399 system. The data shown in each panel are the first 10^5 yr from a 10^8 yr integration.

lines in Figure 4. Many of the unstable regions are the result of the MMR locations shown in Table 2, such as the 1:2 MMR with planet c at 1.10 au, and the 2:1 MMR with planet d at 1.33 au. Even so, there are many islands of stability (albeit narrow) that are present within the HZ, where stable orbits in this context are defined as having survived the full 10^7 yr simulation at that initial semimajor axis (see Section 3.1). Note that these regions of stability mostly lie within the inner half of the HZ, and the outer half of the HZ is dominated by the proximity to planet d. Further note that there is an island of stability centered around the semimajor axis of planet d, allowing for the possibility of Trojan planets (Páez & Efthymiopoulos 2015), for which it is feasible to maintain long-term orbital stability (Cresswell & Nelson 2009; Schwarz et al. 2009).

A 100% survival of the simulation for the injected terrestrial planet does not guarantee long-term stability beyond the 10^7 yr. Given the narrow nature of the stability islands, the long-term stability of the injected planet is highly sensitive to changes in its semimajor axis and/or orbital eccentricity. An example is provided in the bottom panel of Figure 4, which shows the first 10^4 yr of orbital evolution for the injected planet when the starting location is $a = 1.735$ au, corresponding to a very narrow stability spike in the top panel of Figure 4. The eccentricity variations for the injected planet are dominated by a superposition of the perturbing effects of planet c and d (see Figure 2), resulting in an eccentricity amplitude similar to the sum of the planet c and d eccentricity amplitudes. The long-term viability of such a scenario is resolved soon after the 10^7 yr integration, during which an additional simulation revealed the chaotic degradation of the injected planet's orbit and ejection from the system. Although many of the remaining stability islands shown in the top panel of Figure 4 may indeed retain long-term stability, the results presented here demonstrate the uncertain nature of evaluating potential additional orbits within the HZ.

4. Discussion

As described in Section 1, given the relative rarity of giant planets, the HD 141399 system of four giant planets is exceptionally rare among known exoplanetary architectures. According to the NASA Exoplanet Archive (Akeson et al. 2013), HD 141399 is one of only two known planetary systems with at least four planets that are all more massive than Saturn. The other system is HR 8799, with four wide-separation planets that were detected via direct imaging (Marois et al. 2008, 2010). Thus, the HD 141399 system is an incredible

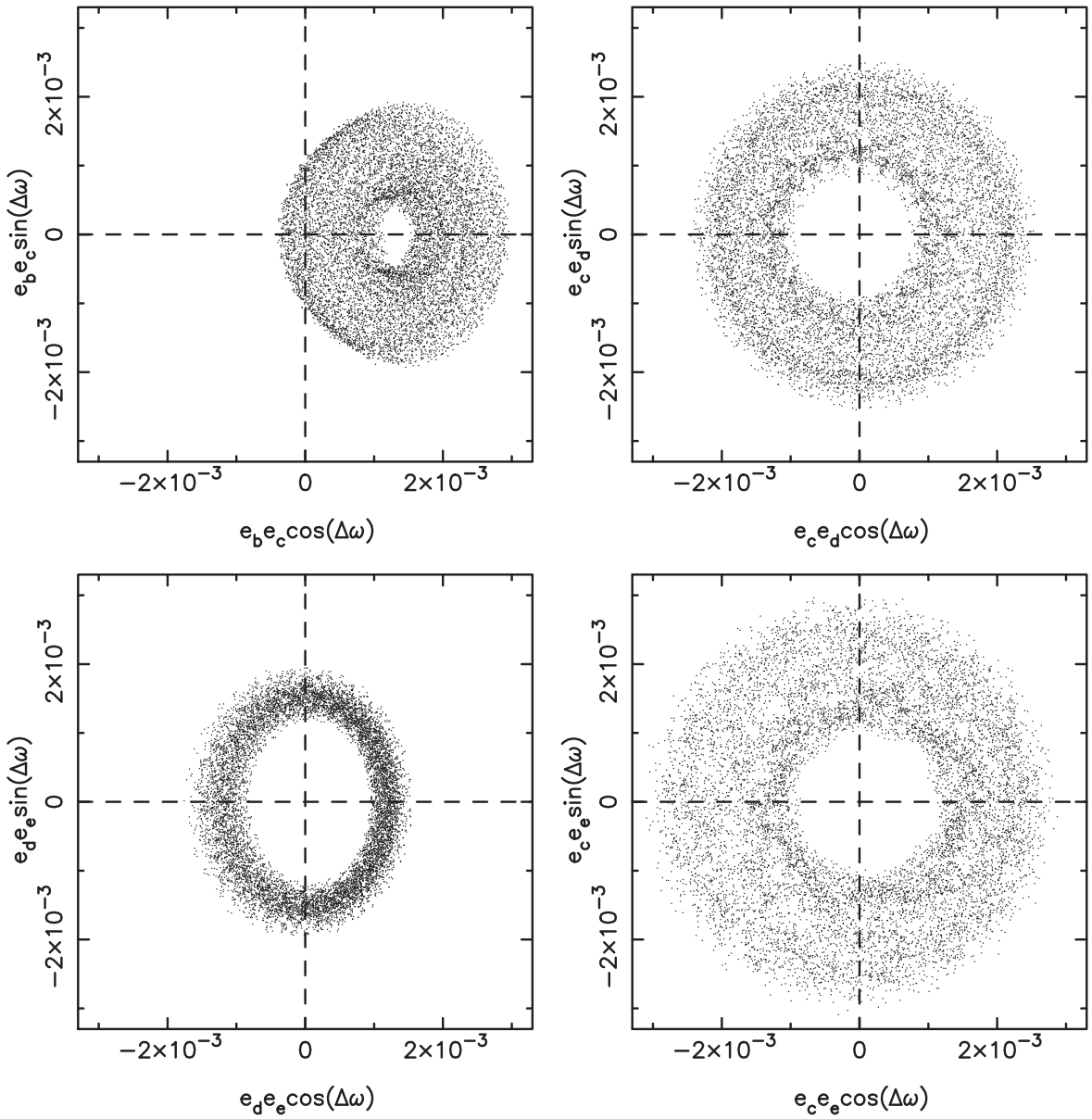

Figure 3. A polar plot of the apsidal trajectory for four planet pairs: b–c (top-left), c–d (top-right), d–e (bottom-left), and c–e (bottom-right). The data in each panel represent the first 10^6 yr of the simulation. The figure shows that the apsidal modes are librating for the b–c planet pair, and are circulating for all other planet pairs.

opportunity to study the formation, dynamics, and evolution of an unusual planetary architecture.

The architecture of the HD 141399 system is known only to the level of completeness of the RV measurements, and additional, as yet undetected, planets may exist within the system. We have now entered the era of extreme precision RV (EPRV) exoplanet searches (Fischer et al. 2016) with the goal of detecting and measuring masses for terrestrial planets. Such efforts have been applied to known exoplanetary systems, such as the recent use of EPRV techniques to detect two additional planets in the rho CrB system (Brewer et al. 2023), a system first discovered by Noyes et al. (1997). In this work, we explored the dynamical feasibility of an Earth-mass planet in the HZ which extends within the range 0.974–2.309 au (see Section 2.1). The semiamplitude of the RV signature for such a planet would be 8.7 cm s^{-1} and 5.6 cm s^{-1} at the inner and outer edges of the HZ, respectively. These amplitudes, like our dynamical simulations, assume a near edge-on inclination for the system. One possible resolution of the inclination ambiguity may lie with an astrometric detection of the outer planet. Through the coming years, the combination of RV and astrometric data will be an increasingly powerful method to characterize non-transiting RV systems (Perryman et al. 2014; Brandt 2021; Winn 2022). Using the orbital parameters provided by Table 1, and the stellar distance of 37.05 pc, the maximum astrometric amplitude of planet e is 0.07 mas. HD 141399 is relatively bright ($V = 7.21$), resulting in the predicted astrometric amplitude for planet e lying well above the Gaia DR3 astrometric precision (Gaia Collaboration et al. 2021; Lindegren et al. 2021).

Indeed, the Hipparcos–Gaia Catalog of Accelerations (Brandt 2021) reveals a moderately significant acceleration of the star from Gaia DR3 astrometry when compared against the constant proper motion model. Although there is no guarantee that the other planets in the system are similarly inclined, an astrometric measurement of the inclination for planet e would

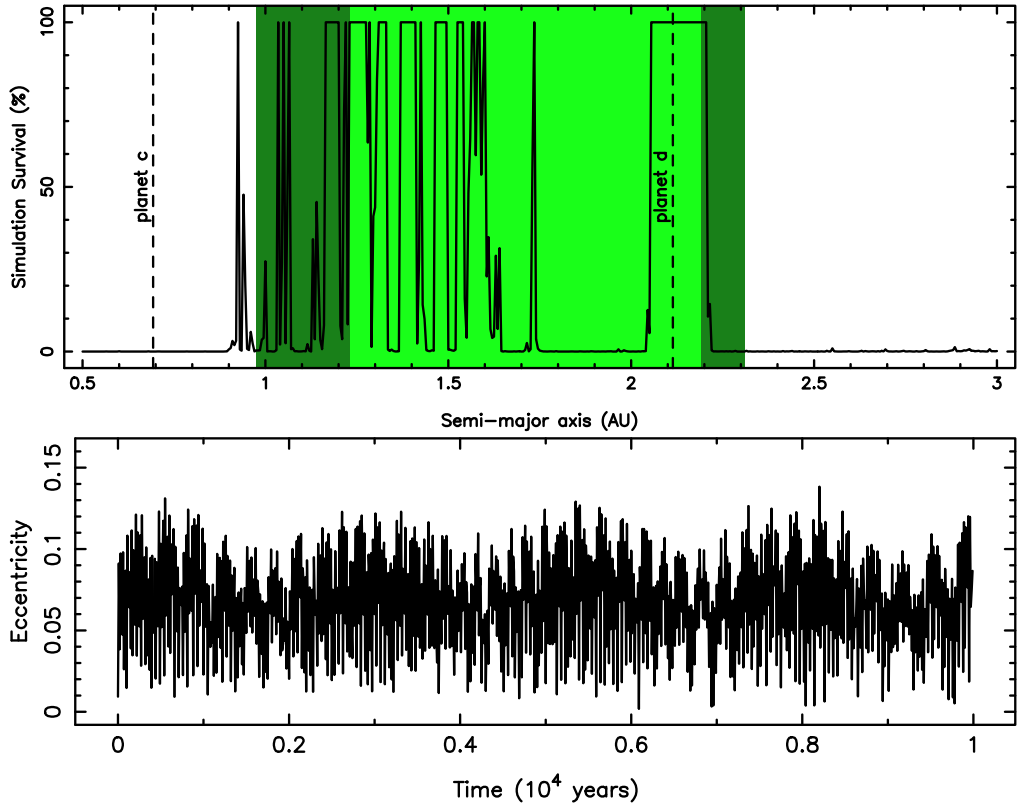

Figure 4. Top: percentage of the simulation that the injected Earth-mass planet survived as a function of semimajor axis, shown as a solid line. As for Figure 1, the CHZ is shown in light green and the OHZ is shown in dark green. The vertical dashed lines indicate the semimajor axes for planets c and d. Bottom: Eccentricity evolution for the injected Earth-mass planet at an initial semimajor axis of 1.735 au.

greatly aid in understanding the formation and evolution of this relatively rare planetary architecture.

Giant planet formation processes that follow the prescription of models such as the "Grand Tack" model for the solar system (e.g., Walsh et al. 2011; Raymond et al. 2014; Nesvorný 2018) suggest disk-dominated giant planet migration occurs prior to the formation of terrestrial planets (e.g., Chambers 2014). Indeed, observation and theoretical evidence supports the proposition that giant planets form and migrate quickly relative to terrestrial planets, thus shaping the architecture of such systems (Pascucci et al. 2006; Raymond et al. 2009; Morbidelli et al. 2012; Clement et al. 2023). This implies that, should terrestrial planets be present in the HZ of HD 141399, they likely formed after the known giant planets, in particular planets c and d either side of the HZ. Such a formation scenario would have significant effects on not only the formation and dynamics of HZ planets, but also their impact history and hydration (O'Brien et al. 2014; Raymond & Izidoro 2017; Sánchez et al. 2018; Bailey & Fabrycky 2022). Thus, it remains uncertain as to the planetary habitability outcome for terrestrial planets within the HD 141399, even if stable orbits can be retained.

It is worth noting that, from the perspective of a terrestrial planet located near the center of the HD 141399 HZ, planet d would provide a spectacular sight. From that perspective, and assuming Jupiter's radius and geometric albedo, planet d would exhibit an apparent visual magnitude of -10 when at opposition, shining more than 5 magnitudes brighter than the maximum brightness of Venus as seen from Earth. Additionally, planet d would have an angular size of $\sim 7'$, which is $\sim$8.5 times larger than Jupiter as seen from Earth, and would easily seen as a disk with the naked eye.

5. Conclusions

As the dominant planetary masses, and considering their relatively rapid formation, giant planets play a pivotal role in the eventual architecture and evolution of systems in which they are present. This is especially important for systems that also contain terrestrial planets, as the habitability of such planets will undoubtedly be influenced by the presence of giant planets within the system. HD 141399 stands as a particularly unusual system with respect to its giant planet inventory, to the point where the pathway to the observed architecture may have effectively suppressed terrestrial planet formation within the system. If indeed there are terrestrial planets that are present within the system HZ, they would serve as useful case studies regarding the influence of giant planets on the prevalence and evolution of surface habitability, such as the role of giant planets in volatile delivery.

The HD 141399 dynamical study presented here provides the results for two main investigations: the stability of the known planets and the viability of a terrestrial planet within the HZ. The results show that the known planets are long-term stable, and that the apsidal trajectories for the b–c planet pair are librating, indicating that they are in or near the 2:1 MMR. Our results for the Earth-mass planet injection simulations show that there are limited islands of stability, and that these islands are sensitive to the initial conditions of the terrestrial planet. The combined angular momentum transfers of planets c and d result in significant eccentricity variations for the injected

planet that can result in an eventual chaotic orbit and loss from the system in some cases. With the progress of RV and astrometric precision, it is hoped that key systems, such as this one, will be observationally revisited in the years ahead to better understand the nature of giant planet systems and their potential to harbor habitable planets in their midst.

Acknowledgments

This research has made use of the Habitable Zone Gallery at hzgallery.org. The results reported herein benefited from collaborations and/or information exchange within NASA's Nexus for Exoplanet System Science (NExSS) research coordination network sponsored by NASA's Science Mission Directorate.

Software: Mercury (Chambers 1999).

ORCID iDs

Stephen R. Kane https://orcid.org/0000-0002-7084-0529

References

Agnew, M. T., Maddison, S. T., Horner, J., & Kane, S. R. 2019, MNRAS, 485, 4703
Akeson, R. L., Chen, X., Ciardi, D., et al. 2013, PASP, 125, 989
Bailey, N. A., & Fabrycky, D. C. 2022, MNRAS, 514, 4765
Barnes, R., & Greenberg, R. 2006a, ApJ, 638, 478
Barnes, R., & Greenberg, R. 2006b, ApJ, 652, L53
Batygin, K. 2015, MNRAS, 451, 2589
Batygin, K., & Morbidelli, A. 2013, AJ, 145, 1
Beaugé, C., Ferraz-Mello, S., & Michtchenko, T. A. 2003, ApJ, 593, 1124
Brandt, T. D. 2021, ApJS, 254, 42
Brewer, J. M., Zhao, L. L., Fischer, D. A., et al. 2023, AJ, 166, 46
Bryan, M. L., Knutson, H. A., Lee, E. J., et al. 2019, AJ, 157, 52
Buchhave, L. A., Bitsch, B., Johansen, A., et al. 2018, ApJ, 856, 37
Carrera, D., Raymond, S. N., & Davies, M. B. 2019, A&A, 629, L7
Chambers, J. 2014, Sci, 344, 479
Chambers, J. E. 1999, MNRAS, 304, 793
Clanton, C., & Gaudi, B. S. 2016, ApJ, 819, 125
Clement, M. S., Deienno, R., & Izidoro, A. 2023, Icar, 389, 115260
Cresswell, P., & Nelson, R. P. 2009, A&A, 493, 1141
Endl, M., Cochran, W. D., Kürster, M., et al. 2006, ApJ, 649, 436
Endl, M., Robertson, P., Cochran, W. D., et al. 2022, AJ, 164, 238
Fernandes, R. B., Mulders, G. D., Pascucci, I., Mordasini, C., & Emsenhuber, A. 2019, ApJ, 874, 81
Fischer, D. A., Anglada-Escude, G., Arriagada, P., et al. 2016, PASP, 128, 066001
Fischer, D. A., & Valenti, J. 2005, ApJ, 622, 1102
Ford, E. B. 2008, AJ, 135, 1008
Ford, E. B. 2014, PNAS, 111, 12616
Ford, E. B., Havlickova, M., & Rasio, F. A. 2001, Icar, 150, 303
Ford, E. B., & Rasio, F. A. 2008, ApJ, 686, 621
Fulton, B. J., Rosenthal, L. J., Hirsch, L. A., et al. 2021, ApJS, 255, 14
Gaia Collaboration, Brown, A. G. A., Vallenari, A., et al. 2018, A&A, 616, A1
Gaia Collaboration, Brown, A. G. A., Vallenari, A., et al. 2021, A&A, 649, A1
Georgakarakos, N., Eggl, S., & Dobbs-Dixon, I. 2018, ApJ, 856, 155
Goldreich, P., & Schlichting, H. E. 2014, AJ, 147, 32
Hadden, S. 2019, AJ, 158, 238
Hébrard, G., Arnold, L., Forveille, T., et al. 2016, A&A, 588, A145
Hill, M. L., Bott, K., Dalba, P. A., et al. 2023, AJ, 165, 34
Hill, M. L., Kane, S. R., Seperuelo Duarte, E., et al. 2018, ApJ, 860, 67
Horner, J., Kane, S. R., Marshall, J. P., et al. 2020, PASP, 132, 102001
Ida, S., & Lin, D. N. C. 2005, ApJ, 626, 1045
Johnson, J. A., Aller, K. M., Howard, A. W., & Crepp, J. R. 2010, PASP, 122, 905
Kane, S. R. 2011, Icar, 214, 327
Kane, S. R. 2019, AJ, 158, 72
Kane, S. R., Arney, G. N., Byrne, P. K., et al. 2021b, JGRE, 126, e06643
Kane, S. R., & Blunt, S. 2019, AJ, 158, 209
Kane, S. R., & Gelino, D. M. 2012, PASP, 124, 323
Kane, S. R., Hill, M. L., Kasting, J. F., et al. 2016, ApJ, 830, 1
Kane, S. R., Li, Z., Wolf, E. T., Ostberg, C., & Hill, M. L. 2021b, AJ, 161, 31
Kane, S. R., & Raymond, S. N. 2014, ApJ, 784, 104
Kane, S. R., Schneider, D. P., & Ge, J. 2007, MNRAS, 377, 1610
Kane, S. R., Turnbull, M. C., Fulton, B. J., et al. 2020, AJ, 160, 81
Kasting, J. F., Whitmire, D. P., & Reynolds, R. T. 1993, Icar, 101, 108
Kopparapu, R. K., & Barnes, R. 2010, ApJ, 716, 1336
Kopparapu, R. K., Ramirez, R., Kasting, J. F., et al. 2013, ApJ, 765, 131
Kopparapu, R. K., Ramirez, R. M., SchottelKotte, J., et al. 2014, ApJ, 787, L29
Levison, H. F., Lissauer, J. J., & Duncan, M. J. 1998, AJ, 116, 1998
Lindegren, L., Klioner, S. A., Hernández, J., et al. 2021, A&A, 649, A2
Marois, C., Macintosh, B., Barman, T., et al. 2008, Sci, 322, 1348
Marois, C., Zuckerman, B., Konopacky, Q. M., Macintosh, B., & Barman, T. 2010, Natur, 468, 1080
Matsumoto, Y., Nagasawa, M., & Ida, S. 2012, Icar, 221, 624
Mishra, L., Alibert, Y., Udry, S., & Mordasini, C. 2023a, A&A, 670, A68
Mishra, L., Alibert, Y., Udry, S., & Mordasini, C. 2023b, A&A, 670, A69
Morbidelli, A., Lunine, J. I., O'Brien, D. P., Raymond, S. N., & Walsh, K. J. 2012, AREPS, 40, 251
Nesvorný, D. 2018, ARA&A, 56, 137
Nielsen, E. L., De Rosa, R. J., Macintosh, B., et al. 2019, AJ, 158, 13
Noyes, R. W., Jha, S., Korzennik, S. G., et al. 1997, ApJL, 483, L111
Obertas, A., Van Laerhoven, C., & Tamayo, D. 2017, Icar, 293, 52
O'Brien, D. P., Walsh, K. J., Morbidelli, A., Raymond, S. N., & Mandell, A. M. 2014, Icar, 239, 74
Páez, R. I., & Efthymiopoulos, C. 2015, CeMDA, 121, 139
Pascucci, I., Gorti, U., Hollenbach, D., et al. 2006, ApJ, 651, 1177
Pass, E. K., Winters, J. G., Charbonneau, D., et al. 2023, AJ, 166, 11
Peale, S. J. 1976, ARA&A, 14, 215
Perryman, M., Hartman, J., Bakos, G. Á, & Lindegren, L. 2014, ApJ, 797, 14
Petrovich, C., Malhotra, R., & Tremaine, S. 2013, ApJ, 770, 24
Raymond, S. N., Barnes, R., Armitage, P. J., & Gorelick, N. 2008, ApJL, 687, L107
Raymond, S. N., & Izidoro, A. 2017, Icar, 297, 134
Raymond, S. N., Kokubo, E., Morbidelli, A., Morishima, R., & Walsh, K. J. 2014, in Protostars and Planets VI, ed. H. Beuther et al. (Tucson, AZ: Univ. Arizona Press), 595
Raymond, S. N., O'Brien, D. P., Morbidelli, A., & Kaib, N. A. 2009, Icar, 203, 644
Rosenthal, L. J., Fulton, B. J., Hirsch, L. A., et al. 2021, ApJS, 255, 8
Sánchez, M. B., de Elía, G. C., & Darriba, L. A. 2018, MNRAS, 481, 1281
Schwarz, R., Süli, Á., Dvorak, R., & Pilat-Lohinger, E. 2009, CeMDA, 104, 69
Vogt, S. S., Butler, R. P., Rivera, E. J., et al. 2014, ApJ, 787, 97
Walsh, K. J., Morbidelli, A., Raymond, S. N., O'Brien, D. P., & Mandell, A. M. 2011, Natur, 475, 206
Winn, J. N. 2022, AJ, 164, 196
Winn, J. N., & Fabrycky, D. C. 2015, ARA&A, 53, 409
Wisdom, J. 2006, AJ, 131, 2294
Wisdom, J., & Holman, M. 1991, AJ, 102, 1528
Wittenmyer, R. A., Butler, R. P., Tinney, C. G., et al. 2016, ApJ, 819, 28
Wittenmyer, R. A., Tinney, C. G., Horner, J., et al. 2013, PASP, 125, 351
Wittenmyer, R. A., Tinney, C. G., O'Toole, S. J., et al. 2011, ApJ, 727, 102
Wittenmyer, R. A., Wang, S., Horner, J., et al. 2020, MNRAS, 492, 377